Chemical Engineering Journal 105 (2005) 81–89

Chemical Engineering Journal

www.elsevier.com/locate/cej

# Fluidized bed combustion and desulfurization of a heavy liquid fuel

Francesco Miccio[a,*], Farouk M. Okasha[b]

[a] *Istituto di Ricerche sulla Combustione, CNR, via Metastasio 17, 80125 Napoli, Italy*
[b] *Department of Mechanical Engineering, Faculty of Engineering, Mansoura University, Egypt*

Received 5 July 2004; received in revised form 6 September 2004; accepted 5 October 2004

**Abstract**

An experimental and theoretical study on the combustion and desulfurization of liquid fuels in fluidized beds is proposed in the paper.

Tests with a high sulfur liquid fuel (Egyptian mazut) have been performed in a bubbling fluidized bed combustor equipped with a special fuel injector at different operating conditions. Limestone is used as sorbent at various Ca/S ratio. The experiments evidenced that efficient combustion and desulfurization can be achieved under operating conditions that maximize the mixing of fuel vapors and bed materials and depress the spontaneous formation of endogenous fuel rich bubbles. A tall bed and high fuel dispersion velocity largely improve the process efficiency. The design and operation of the fuel feeding device also have a key role.

The theoretical study was aimed at developing a predictive model for estimating the desulfurization efficiency in a fluidized bed fed with liquid fuels. The model is based on a novel three phases schematization of the bed. It accounts for the mechanism of bubble coalescence, the diffusion between bubbles and the emulsion, the sulfation reaction, the sorbent attrition and elutriation. A macro-kinetics of fuel oxidation is adopted for the prediction of the $O_2$ partial pressure in the bed. Model results are presented in the paper. The trend and the measured values obtained from the experiments are well predicted by the model, even if some refinements are needed in order to have a very accurate estimation of the sulfur retention.


*Keywords:* Desulfurization; Fluidized bed combustion; Heavy liquid fuels

## 1. Introduction

During the last decades, market value of heavy oil fuels with high sulfur content has been gradually shrunken because of the more stringent regulations on noxious emissions. Such fuels are regarded as a source of serious environmental difficulties when burned in conventional furnaces due to the high level of sulfur dioxide in flue gases. Alternatively, these fuels can be reliably processed using fluidized bed (FB) combustion thanks to its robustness, flexibility and effectiveness [1], whilst meeting environmental standards on pollutant emissions, with particular concern to in situ desulfurization. This trend has more sound when coupled with the actuality that the quality of the crude oil produced worldwide is steadily deteriorating. In other words, the crude oil is gradually becoming heavier with higher sulfur content [2].

Little research activities have been carried out on FB combustion of liquid fuels. In pioneer works a number of difficulties were encountered including cracking, bed agglomeration, injector blocking, post-burning in freeboard, non-uniform temperature distribution, unacceptable combustion and desulfurization efficiencies [3–6]. However, most of the above problems have been overcome thanks to the optimization of the operating conditions and a good design of the fuel injection system that represents a key element for the successful operation of the combustor. A number of liquid fuels have been efficiently burned in fluidized beds including acid tar, heavy fuel oil, kerosene, pyrolysis oil, bitumen-based emulsion, gas–oil, asphalt [7–11]. High sulfur retention, up to 95%, was attained by feeding sorbent particles, but this performance strongly depends on the adopted Ca/S ratio (typically 3–5).

* Corresponding author. Tel.: +39 08 15931567; fax: +39 08 15931567.
*E-mail addresses:* miccio@irc.cnr.it (F. Miccio), faroukok@mans.edu.eg (F.M. Okasha).

1385-8947/$ – see front matter © 2004 Elsevier B.V. All rights reserved.
doi:10.1016/j.cej.2004.10.001

**Nomenclature**

| | |
|---|---|
| $a$ | $O_2$ exponent in the reaction rate equation for fuel oxidation (–) |
| AFR | air fuel ratio at the injector (–) |
| $b$ | fuel exponent in the reaction rate equation for fuel oxidation (–) |
| $C$ | $SO_2$ concentration (mol m$^{-3}$) |
| $C_g$ | overall gas concentration (mol m$^{-3}$) |
| $d_0$ | nozzle size of the fuel injector (m) |
| $D$ | bubble diameter (m) |
| $D_p$ | particle size (m) |
| $D_t$ | combustor diameter (m) |
| $f$ | bubble frequency (Hz) |
| $g$ | gravity acceleration (m s$^{-2}$) |
| $k_{ox}$ | rate of fuel oxidation (mol m$^{-3}$ s$^{-1}$) |
| $K_a$ | attrition constant (–) |
| $K_{be,i}$ | coefficient of mass transfer between bubbles and emulsion (s$^{-1}$) |
| $K_{bc,i}$ | coefficient of mass transfer between bubbles and cloud (s$^{-1}$) |
| $K_{ce,i}$ | coefficient of mass transfer between cloud and emulsion (s$^{-1}$) |
| $K_1$ | rate of sulfation reaction (m$^3$ mol$^{-1}$ s$^{-1}$) |
| $K_2$, $K_3$ | exponential. parameters for sulfation kinetics (–) |
| $L$ | bed height (m) |
| $L^*$ | static bed height (m) |
| $\dot{m}_f$ | mass flow rate of the fuel (kg s$^{-1}$) |
| $M_f$ | molecular weight of the fuel (kg mol$^{-1}$) |
| $p_{O_2}$ | partial pressure of $O_2$ in the emulsion (–) |
| $P$ | pressure (Pa) |
| $Q$ | volumetric flow rate (m$^3$ s$^{-1}$) |
| $R$ | kinetic rate of sulfation (m$^3$ mol$^{-1}$ s$^{-1}$) |
| $R_g$ | gas-law constant (J mol$^{-1}$ K$^{-1}$) |
| $S$ | bed section (m$^3$) |
| $T$ | bed temperature (K) |
| $T_0$ | room temperature (K) |
| $u_0$ | dispersion velocity (m s$^{-1}$) |
| $U$ | fluidization velocity (m s$^{-1}$) |
| $U_{br,i}$ | rising velocity of a single bubble (m s$^{-1}$) |
| $U_{ed}$, $U_{ex}$ | bubble rising velocities (m s$^{-1}$) |
| $U_{mf}$ | minimum fluidization velocity (m s$^{-1}$) |
| $W$ | sorbent load in the bed (mol) |
| $X_S$ | sulfur content in the fuel (–) |
| $z$ | elevation (m) |

*Greek letters*

| | |
|---|---|
| $\alpha$ | stoichiometric coefficient (–) |
| $\gamma$ | fuel concentration (mol m$^{-3}$) |
| $\varepsilon$ | bubble hold-up in the bed (–) |
| $\eta$ | desulfurization efficiency (–) |
| $\eta_c$ | combustion efficiency (%) |
| $\vartheta$ | $O_2$ concentration (mol m$^{-3}$) |
| $\xi$ | conversion degree (–) |
| $\Psi$ | Ca/S molar ratio (–) |
| $\Omega$ | $SO_2$ diffusivity (m$^2$ s$^{-1}$) |

*Subscripts*

| | |
|---|---|
| ed | endogenous phase |
| em | emulsion phase |
| ex | exogenous phase |

The desulfurization during fluidized bed combustion of coals and other solid fuels is a well established process [12]. The sulfur is released during both devolatilization and char combustion, leading to good mixing between gaseous sulfur species and sorbent particles in the bed. Since FB desulfurization is based on a heterogeneous reaction; the process is not efficient when a poor contact between sorbent particles and gaseous sulfur species occurs. In general, factors that limit internal mixing of reactants affect the desulfurization. Another source of disturbance is the periodic change between oxidizing and reducing conditions, which are likely to occur inside a fluidized bed [12,13]. The alternating exposure of the calcareous materials to different reactive atmospheres induces cycles of sulfur adsorption or release from sorbent particles, and, on the whole, may significant affect the performance of the reactor. As far as liquid fuels are concerned, the mechanism of combustion and sulfur release is quite different with respect to coal. The fuel is normally fed by means of lateral ports where fuel rich regions are generated. In addition fuel evaporation and pyrolysis are very fast and, in turn, bubbles containing fuel vapors are formed. It is known that segregation phenomena are responsible of low in-bed conversion of volatile matters generated during early stages of FB combustion of high-volatile solid fuels [14]. In fact, fuel rich bubbles escape the bed and burn in the freeboard; this takes place irrespectively of the fuel nature (solid, liquid or gas). The formation of fuel rich regions in the proximity of the injector during FB combustion of liquid fuels, leads to the formation and periodical detachment of "endogenous" bubbles as a result of fuel dispersion and evaporation [15].

The present paper is a contribution to better understand the mechanisms of combustion and desulfurization of liquid fuels. This aim is pursued on the base of purposely developed experiments that are intended to explore the connection between the efficiency of combustion and desulfurization. In order to well understand the observed phenomenology a theoretical study is also proposed aiming at developing a mathematical model of desulfurization, applicable to liquid fuels. The model presents some innovative aspects concerning the mechanism of interaction between the different phases under which a fluidized bed can be schematized. The results

of the model are presented in the paper and compared with experimental data.

## 2. Experimental

### *2.1. Description of the experimental facility and materials*

Steady state combustion tests were carried out in a bubbling fluidized bed located in Mansoura. A scheme of the experimental facility is reported in Fig. 1. The fluidization column has an inner diameter of 300 mm and a total height of 3300 mm. Details of the apparatus can be found elsewhere [16]. The primary air stream is introduced at the bottom of the fluidization column, by means of an air distributor provided with 68 vertical nozzles. Silica sand with a narrow size distribution (0.5–0.8 mm) is used as bed material. The combustor is equipped with a number of probes for temperature measurements in radial and axial directions based on type K thermocouples connected with a multipoint temperature recorder. The rate of primary air is measured using a calibrated diaphragm whereas the dispersing air rate is measured by a rotameter. A TESTO 350 gas analyzer is used for measurements of $O_2$, $CO_2$, CO, $SO_2$ and $NO_x$ concentration in the flue gas.

The liquid fuel is introduced at the bottom of the bed by means of a pump connected to a pneumatic injector, which is vertically mounted at the centerline of the distributor. The injector mainly consists of two coaxial tubes, as shown in Fig. 2. The liquid fuel is passed in the inner tube then proceeds to the annulus while a dispersing air stream is fed into the annulus to entrain fuel droplets. Finally, the dispersed fuel is discharged into the fluidized bed via eight lateral nozzles at the top of the injector. The ratio between the dispersing air rate and the fuel feeding rate is denoted as AFR. Both primary and dispersing air streams are considered for the calculation of the fluidization velocity and excess air ratio.

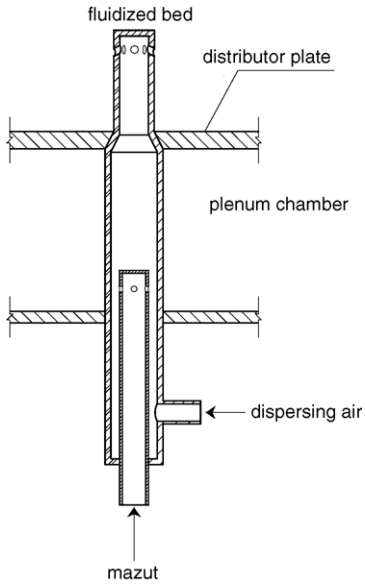


Fig. 2. The vertical injector for liquid fuels.

The fuel is a heavy oil (Egyptian mazut), having no oxygen and around 3.2% of sulfur content. Its properties are reported in Table 1. The fluidization velocity, the excess air ratio and the bed temperature are fixed at 1.0 m s$^{-1}$, 1.3 and 850 °C, respectively. Different static bed heights ($L^*$) are adopted during the experiments (0.3–0.5 m). The ratio between mass flow rates of the dispersing air and fuel (AFR) at

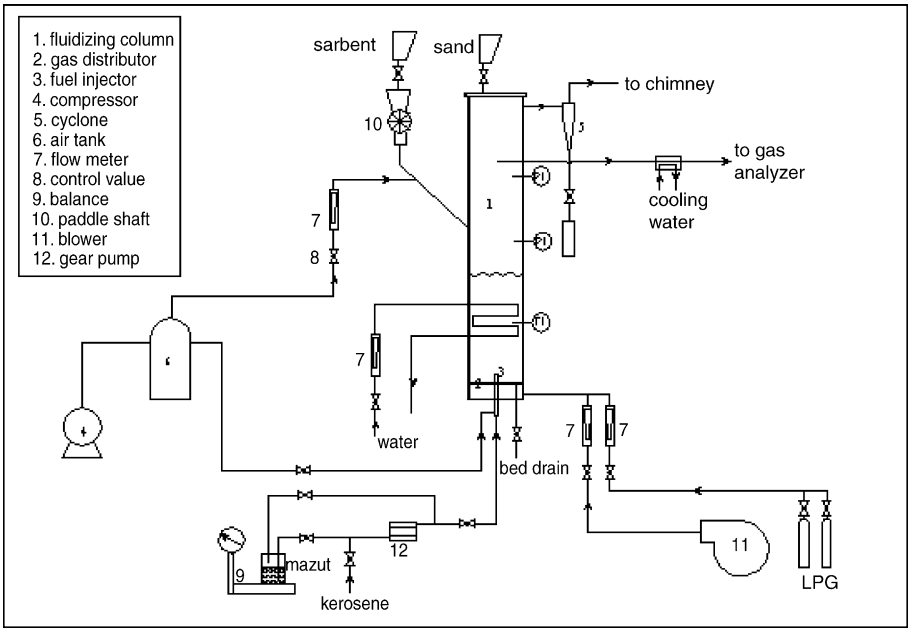


Fig. 1. A scheme of the experimental facility.

Table 1
Fuel properties

| | |
|---|---|
| Density (at 15 °C) (kg m$^{-3}$) | 946 |
| Water content, % by mass | 0.2 |
| Low heating value (dry base) (MJ kg$^{-1}$) | 40.7 |
| Elemental analysis (dry base) | |
| Carbon, % by mass | 84.8 |
| Hydrogen, % by mass | 11.6 |
| Nitrogen, % by mass | 0.3 |
| Sulfur, % by mass | 3.2 |
| Ashes, % by mass | 0.1 |

the injector is also varied in the range 1–5. The sulfur capture is accomplished by continuously feeding Borg-El-Arab limestone (0.65 mm size). The limestone is composed of calcium carbonate (92.47%), magnesium carbonate (3.20) and inert (4.33) on dry basis. The molar ratio $\Psi$ between Ca and S was varied in the range 0–5.

## 3. Results

The experimental results are presented in Table 2 in terms of CO and $NO_x$ emissions and combustion efficiency ($\eta_c$). The maximum combustion efficiency (99.8%) is achieved at the higher values of bed height and AFR. The influence of bed height is straightforward, because increasing $L^*$ leads to a longer residence time of the fuel vapors in the bed. Also the augmentation of AFR is beneficial for CO reduction and efficiency improvement. This can be ascribed to the relevant role played by AFR in promoting the fuel atomization and the mixing between air and fuel vapors. The $NO_x$ concentration is limited at around 100 ppm and a small change can be noted (20 ppm) when operating conditions are varied, due to the reducing action of CO.

Fig. 3 reports the desulfurization efficiency ($\eta$) versus the Ca/S ratio ($\Psi$) for tests at different values of the bed height and AFR. Again, it appears that conditions favorable for achieving an efficient combustion also promote the sulfur capture in the bed. The higher the bed, the larger is sulfur retention. The result is again ascribed to the increased residence time of the gases in the bed. Thus, the contact time between $SO_2$ and sorbent particles is improved and a larger $SO_2$ retention is achieved.

Table 2
Experimental results

| $T$ (°C) | $L^a$ (m) | AFR | CO (ppm) | $NO_x$ (ppm) | $O_2$ (%) | $\eta_c$ (%) |
|---|---|---|---|---|---|---|
| 850 | 0.30 | 4 | 1066 | 94 | 5.51 | 97.8 |
| 850 | 0.40 | 4 | 431 | 99 | 5.23 | 99.1 |
| 850 | 0.50 | 4 | 143 | 103 | 5.11 | 99.7 |
| 850 | 0.5 | 1 | 770 | 84 | 5.38 | 98.4 |
| 850 | 0.5 | 2 | 527 | 88 | 5.27 | 98.9 |
| 850 | 0.5 | 3 | 286 | 94 | 5.18 | 99.4 |
| 850 | 0.5 | 4 | 143 | 103 | 5.11 | 99.7 |
| 850 | 0.5 | 5 | 103 | 106 | 5.06 | 99.8 |

Excess air factor: 1.3.
[a] Static bed height.

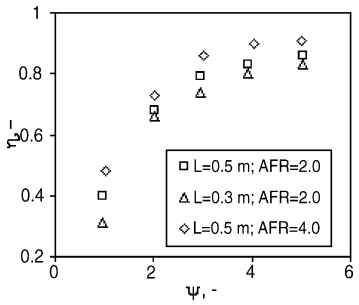


Fig. 3. Desulfurization efficiency vs. Ca/S ratio in experiments carried out at $T = 850$ °C and $U = 1.0$ m s$^{-1}$.

As already observed for the combustion efficiency, the sulfur retention also augments with increasing the dispersing air flow rate. This is a consequence of a better fuel atomization and a more intimate mixing between gaseous sulfur species ($H_2S$ and $SO_2$) and sorbent particles inside the bed. On this concern, the design and the location of the fuel injector seem to be very effective.

Similar to coal-based processes, the calcium to sulfur molar feed ratio has a large impact on the desulfurization efficiency. Increasing $\Psi$ in the range 0–3.5 results in a greater $SO_2$ removal (Fig. 3), after that an asymptotic value is attained and a further increase of $\Psi$ is less effective. In contrast, the sorbent conversion is progressively reduced moving toward a higher sorbent excess.

## 4. Modeling

The sulfur retention and sorbent conversion in a steady state and isothermal bubbling FB combustor was evaluated by developing a mathematical model based on the two phases theory of the fluidization [17]. This model derives from the merging and upgrade of two previous ones concerning the fluidized bed desulfurization of high-volatiles fuels [18] and the dispersion and coalescence of fuel rich bubbles [15]. With reference to Fig. 4A, which gives a sketch of the bed zone considered in this theoretical framework, three distinct phases are considered inside the bed:

(i) an emulsion phase (em) made of bed materials at minimum fluidization;
(ii) an exogenous bubble phase (ex) made by air bubbles formed at the distributor;
(iii) an endogenous bubble phase (ed) made by fuel rich bubbles formed at the fuel inlet port.

The emulsion phase is assumed perfectly mixed whereas both bubble phases behave as plug flow reactors (see Fig. 4B).

The following assumptions are made:

(i) Sulfur is rapidly released in endogenous bubbles as sulfur dioxide.

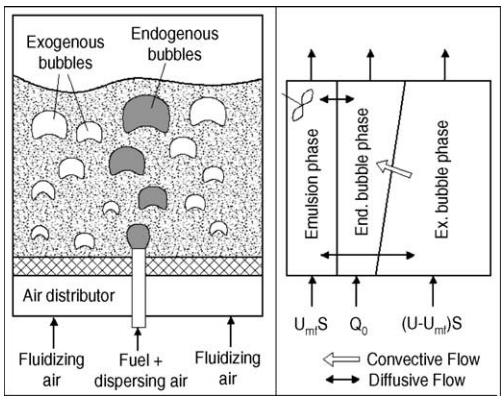


Fig. 4. A sketch of the bed zone with the fuel injector (A) and the schematization of the three phases considered by the model (B).

(ii) Diffusive mass transfer occurs between the emulsion phase and both bubble phases.
(iii) The size of exogenous bubbles increases by coalescence according to Cai et al. [19].
(iv) An endogenous bubble may capture by coalescence exogenous ones during its lift-up.
(v) The desulfurization in the bubble phases and in the freeboard region is negligible.
(vi) The sulfation kinetics depends on the partial pressure of $SO_2$ and $O_2$ as well as on the sorbent conversion degree.
(vii) The sorbent hold-up in the bed and its conversion degree attains a constant value at steady state.

It is worth noting that the knowledge of the $O_2$ partial pressure in the emulsion phase is strictly required (assumption (vi)) and, consequently, a combustion model for fuel vapors is needed. To this aim, a simplified kinetic scheme valid for oxidation of gaseous hydrocarbons in the temperature range 960–1540 K has been applied. It is based on a single step global rate equation:

$$\text{fuel} + \alpha O_2 \rightarrow \text{products}$$

as reported by Westbrook and Dryer [20]. In addition, the fuel vapors are assumed to be produced very quickly upon liquid fuel injection.

Eq. (1) provides the relationship between the volumetric flow rate $Q_{ed}$, frequency $f_{ed}$ and size $D_{ed}$ of endogenous bubbles

$$Q_{ed} = f_{ed}\tfrac{1}{6}(\pi)D_{ed}^3 \tag{1}$$

Since no coalescence occurs between endogenous bubbles, their frequency is constant (Eq. (2)) along the axial coordinate $z$

$$\frac{d}{dz}f_{ed} = 0 \tag{2}$$

Eq. (3) is the continuity equation for the volumetric flow rates of exogenous and endogenous phases

$$\frac{d}{dz}Q_{ed} = -\frac{d}{dz}Q_{ex} \tag{3}$$

The species conservation equations of $SO_2$ are given by Eqs. (4) and (5), for exogenous and endogenous phases respectively

$$\frac{d}{dz}Q_{ex}C_{ex} = S\varepsilon_{ex}K_{be,ex}(C_{em} - C_{ex}) + C_{ex}\frac{dQ_{ex}}{dz} \tag{4}$$

$$\frac{d}{dz}Q_{ed}C_{ed} = S\varepsilon_{ed}K_{be,ed}(C_{em} - C_{ed}) - C_{ex}\frac{dQ_{ex}}{dz} \tag{5}$$

It is worth noting that the last term of Eqs. (3) and (4) is identical and represents the net convective flow due to the coalescence between bubbles of different phases.

For the exogenous phase, the species conservation equations of $O_2$ and fuel are given by Eqs. (6a) and (6b) that include the generation rate by chemical reaction (last term)

$$\frac{d}{dz}Q_{ex}\vartheta_{ex} = S\varepsilon_{ex}K_{be,ex}(\vartheta_{em} - \vartheta_{ex}) + \vartheta_{ex}\frac{dQ_{ex}}{dz} - S\alpha k_{ox}\frac{\gamma_{ex}^a}{C_g}\frac{\vartheta_{ex}^b}{C_g} \tag{6a}$$

$$\frac{d}{dz}Q_{ex}\gamma_{ex} = S\varepsilon_{ex}K_{be,ex}(\gamma_{em} - \gamma_{ex}) + \gamma_{ex}\frac{dQ_{ex}}{dz} - Sk_{ox}\frac{\gamma_{ex}^a}{C_g}\frac{\vartheta_{ex}^b}{C_g} \tag{6b}$$

where $\vartheta$ and $\gamma$ are the molar concentration of $O_2$ and fuel, $C_g = P/R_gT$ is the overall gas concentration, $\alpha$ the stoichiometric coefficient of the fuel oxidation reaction.

Similarly, the species conservation equations of $O_2$ and fuel in the endogenous phase were worked out (Eqs. (7a) and (7b))

$$\frac{d}{dz}Q_{ed}\vartheta_{ed} = S\varepsilon_{ed}K_{be,ed}(\vartheta_{em} - \vartheta_{ed}) - \vartheta_{ex}\frac{dQ_{ex}}{dz} + S\alpha k_{ox}\frac{\gamma_{ed}^a}{C_g}\frac{\vartheta_{ed}^b}{C_g} \tag{7a}$$

$$\frac{d}{dz}Q_{ed}\gamma_{ed} = S\varepsilon_{ed}K_{be,ed}(\gamma_{em} - \gamma_{ed}) - \gamma_{ex}\frac{dQ_{ex}}{dz} + Sk_{ox}\frac{\gamma_{ed}^a}{C_g}\frac{\vartheta_{ed}^b}{C_g} \tag{7b}$$

The coefficient of mass transfer $K_{be,i}$ between a generic bubble ($i$ = ed, ex) and the emulsion is evaluated by means of Eqs. (8)–(10) [17]

$$K_{be,i} = \left(\frac{1}{K_{bc,i}} + \frac{1}{K_{ce,i}}\right)^{-1} \tag{8}$$

$$K_{\mathrm{bc},i} = 4.5\frac{U-U_{\mathrm{mf}}}{D_i} + 5.85\frac{\Omega^{1/2}g^{1/4}}{D_i^{5/4}} \tag{9}$$

$$K_{\mathrm{ce},i} = 6.78\sqrt{\frac{\varepsilon_{\mathrm{mf}}\Omega U_i}{D_i^3}} \tag{10}$$

Eq. (11) accounts for the incremental rate of the endogenous bubble size upon coalescence with exogenous bubbles [15]

$$\frac{\mathrm{d}}{\mathrm{d}z}D_{\mathrm{ed}} = \frac{|U_{\mathrm{ex}}-U_{\mathrm{ed}}|\,(D_{\mathrm{ex}}+D_{\mathrm{ed}})^2}{2U_{\mathrm{ed}}D_{\mathrm{ed}}^2}\varepsilon_{\mathrm{ex}} \tag{11}$$

The size of exogenous bubbles is calculated as a function of the elevation and $U-U_{\mathrm{mf}}$ by means of the correlation (Eq. (12)) proposed by Cai et al. [19]

$$D_{\mathrm{ex}} = 0.38(U-U_{\mathrm{mf}})^{0.42}z^{0.8} \exp[-0.25(U-U_{\mathrm{mf}})^2 - 0.1(U-U_{\mathrm{mf}})] \tag{12}$$

The hold-up and the rising velocity of both exogenous and endogenous bubbles ($i$ = ed, ex) are calculated via Eqs. (13) and (14), respectively [17]

$$\varepsilon_i = \frac{U-U_{\mathrm{mf}}}{U-U_{\mathrm{mf}}+U_i} \tag{13}$$

$$U_i = 1.6[(U-U_{\mathrm{mf}}) + 1.13\sqrt{D_i}]D_t^{1.35} + U_{\mathrm{br},i} \tag{14}$$

where

$$U_{\mathrm{br},i} = 0.711\sqrt{gD_i} \quad \text{for}\ \frac{D_i}{D_T} < 0.125 \tag{15}$$

$$U_{\mathrm{br},i} = 0.711\sqrt{gD_i}\,1.2\exp\left(-1.49\frac{D_i}{D_t}\right) \quad \text{for}\ 0.125 < \frac{D_i}{D_T} < 0.6 \tag{16}$$

$$U_{\mathrm{br},i} = 0.35\sqrt{gD_i} \quad \text{for}\ \frac{D_i}{D_T} > 0.6 \tag{17}$$

The species conservation equation of $SO_2$ in the emulsion phase is given in integral form by Eq. (18)

$$RWC_{\mathrm{em}} + U_{\mathrm{mf}}SC_{\mathrm{em}} + S\int_0^L [\varepsilon_{\mathrm{ed}}K_{\mathrm{be,ed}}(C_{\mathrm{ed}}-C_{\mathrm{em}}) + \varepsilon_{\mathrm{ex}}K_{\mathrm{be,ex}}(C_{\mathrm{ex}}-C_{\mathrm{em}})]\,\mathrm{d}z = 0 \tag{18}$$

where the kinetic rate of the sulfation reaction at $T = 850\,^{\circ}\mathrm{C}$ depends via Eq. (19) on the $O_2$ partial pressure $p_{O2}$ and the sorbent conversion degree $\xi$

$$R = K_1\exp(-K_2\xi)p_{\mathrm{O_2}}^{0.5}\exp(-K_3p_{\mathrm{O_2}}) \tag{19}$$

Similar integral equations (Eqs. (20a) and (20b)) account for the species conservation of $O_2$ and fuel in the emulsion phase, provided that the hydrocarbon conversion in the emulsion is negligible [21]

$$U_{\mathrm{mf}}S(\vartheta_{\mathrm{em}}-\vartheta_0) + S\int_0^L [\varepsilon_{\mathrm{ed}}K_{\mathrm{be,ed}}(\vartheta_{\mathrm{ed}}-\vartheta_{\mathrm{em}}) + \varepsilon_{\mathrm{ex}}K_{\mathrm{be,ex}}(\vartheta_{\mathrm{ex}}-\vartheta_{\mathrm{em}})]\,\mathrm{d}z = 0 \tag{20a}$$

$$U_{\mathrm{mf}}S(\gamma_{\mathrm{em}}) + S\int_0^L [\varepsilon_{\mathrm{ed}}K_{\mathrm{be,ed}}(\gamma_{\mathrm{ed}}-\gamma_{\mathrm{em}}) + \varepsilon_{\mathrm{ex}}K_{\mathrm{be,ex}}(\gamma_{\mathrm{ex}}-\gamma_{\mathrm{em}})]\,\mathrm{d}z = 0 \tag{20b}$$

The mass balance for the sorbent in the bed at steady state reads:

$$\frac{\dot{m}_{\mathrm{f}}X}{0.032}\psi = WK_{\mathrm{a}}\frac{U-U_{\mathrm{mf}}}{D_{\mathrm{p}}} \tag{21}$$

where the sorbent feeding rate is equated to the generation rate of elutriable fines. The latter is proportional by means of the attrition constant $K_a$ to the sorbent load in the bed ($W$), the excess velocity above minimum for fluidization ($U-U_{\mathrm{mf}}$) and the inverse of particle size ($1/D_p$) [20].

The sulfur retention and the sorbent conversion degree are defined by Eqs. (22) and (23), respectively

$$\eta = 1 - \frac{SU_{\mathrm{mf}}C_{\mathrm{em}} + Q_{\mathrm{ed}}C_{\mathrm{ed}|z=L} + Q_{\mathrm{ex}}C_{\mathrm{ex}|z=L}}{\dot{m}_{\mathrm{f}}X/0.032} \tag{22}$$

$$\xi = \frac{\eta}{\psi} \tag{23}$$

The system of differential, integral and algebraic equations is integrated under the following initial conditions ($z = 0$):

$$C_{\mathrm{ex}|z=0} = 0$$

$$C_{\mathrm{ed}|z=0} = \frac{X_{\mathrm{S}}}{0.032}\frac{\dot{m}_{\mathrm{f}}}{Q_{\mathrm{disp}}}$$

$$\vartheta_{\mathrm{ex}|z=0} = 0.21\frac{P}{R_{\mathrm{g}}T}$$

$$\vartheta_{\mathrm{ed}|z=0} = \frac{0.21\,u_0(\pi d_0^2/4)(P/R_{\mathrm{g}}T_0)}{Q_{\mathrm{ed}|z=0}}$$

$$\gamma_{\mathrm{ex}|z=0} = 0$$

$$\gamma_{\mathrm{ed}|z=0} = \frac{\dot{m}_{\mathrm{f}}(1-X_{\mathrm{S}})/M_{\mathrm{f}}}{Q_{\mathrm{ed}|z=0}}$$

$$Q_{\mathrm{ex}|z=0} = S(U-U_{\mathrm{mf}})$$

$$Q_{\mathrm{ed}|z=0} = u_0\frac{\pi d_0^2}{4}\frac{T}{T_0} + \frac{\dot{m}_{\mathrm{f}}(1-X_{\mathrm{S}})}{M_{\mathrm{f}}}\frac{R_{\mathrm{g}}T}{P}$$

$$D_{\mathrm{ex}|z=0} = D_{\mathrm{ex},0}$$

Table 3
Input variables of the model

| | |
|---|---|
| Temperature (°C) | 850 |
| Bed diameter (m) | 0.3 |
| Bed height (m) | 0.3–0.9 |
| Particle size (mm) | 0.7 |
| Fuel rate (kg s$^{-1}$) | $1.6 \times 10^{-3}$ |
| Fluidization velocity (m s$^{-1}$) | 1.0 |
| Minimum fluidization velocity (m s$^{-1}$) | 0.17 |
| AFR (–) | 1.7–3.1 |
| Bed voidage at minimum fluidization (–) | 0.48 |
| Sulfur content in the fuel (%) | 3.2 |
| Ca/S molar ratio (–) | 1–5 |
| Sulfation kinetic constant (m$^3$ mol$^{-1}$ s$^{-1}$) | 0.384 |
| Sulfation kinetic exponent, $K_2$ (–) | 10 |
| Sulfation kinetic exponent, $K_3$ (–) | 3 |
| Stoichiometric coefficient $\alpha$ (–) | 13.3 |
| Oxidation kinetic constant, $R_{ox}$ (mol m$^{-3}$ s$^{-1}$) | $5.52 \times 10^5$ |
| Oxidation exponent, $a$ (–) | 0.25 |
| Oxidation exponent, $b$ (–) | 1.5 |
| Attrition constant (–) | $6.7 \times 10^{-8}$ |
| Gas diffusivity coefficient (m$^2$ s$^{-1}$) | $7.0 \times 10^{-5}$ |

$$D_{ed|z=0} = \left\{ \frac{6}{\pi} 1.138 \left( u_0 \frac{\pi d_0^2}{4} + \frac{\dot{m}_f (1 - X_S)}{M_f} \frac{R_g T_0}{P} \right)^{1.2} g^{-0.6} \frac{T}{T_0} \right\}^{1/3}$$

The last condition is the Davidson and Schuler equation [17] upon correction for the gas expansion due to temperature rise in the bed.

Since the oxygen depletion in the emulsion by sulfur capture is negligible, the solution of species conservation equations for $O_2$ and fuel can be decoupled from the $SO_2$ conservation equations. Thus, a first iterative step of the numerical model computes the $O_2$ partial pressure in the emulsion, as well as concentration profiles in endogenous and exogenous phases. In a second step, an iterative procedure has been implemented by means of two nested cycles of iterations for $SO_2$ concentration in the emulsion phase and the sorbent conversion degree.

Input variables of the model are listed in Table 3. Their values are taken from the literature [15,18,20,22] and well reproduce typical conditions of the experiments. The parameters for the sulfatation kinetics of Borg-El-Arab limestone were experimentally evaluated at bench scale following a procedure similar to that adopted by Scala et al. [22]. A base case of calculations is assumed for $L = 0.9$ m, $\Psi = 3$ and AFR = 1.7.

## 5. Model results and discussion

The model estimates of the $O_2$ partial pressure in the emulsion are in the range 0.06–0.10, indicating that the emulsion phase is far from reducing conditions. Nevertheless it cannot be excluded that reducing condition are locally established, by the occurrence of fuel rich flames that percolate through the emulsion phase.

Figs. 5–7 report the profiles along the combustor axial coordinate $z$ of the bubble diameters, the coefficients of mass transfer and the $SO_2$ concentration, respectively. Calculations are made for the base case. Fig. 5 shows that the size of the exogenous bubbles increases more rapidly than endogenous bubbles. The transition from bubbling to slugging regime of fluidization takes place at the elevation of about 0.6 m, corresponding to a bubble size of around 0.2 m. As far as endogenous phase is concerned, its final sizes is comparable to the initial one, the net increase being limited under 40% of the initial size. As a consequence of the different increasing rate between endogenous and exogenous bubble sizes, the coefficient of mass transfer is also subjected to a very different evolution. It clearly appears from analysis of Fig. 6 that $K_{be}$ falls down of two orders of magnitude for the exogenous phase whereas it decreases from 1.8 to 1.0 s$^{-1}$ for the endogenous phase. The profiles of the $SO_2$ concentration (Fig. 7) for endogenous and exogenous phases asymptotically tend moving along the combustor axis to the constant value attained in the emulsion. The $SO_2$ concentration in endogenous bubbles

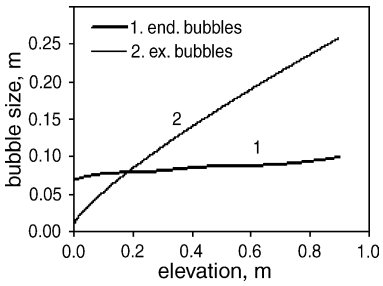


Fig. 5. Bubble size vs. combustor elevation for endogenous and exogenous phases (base case of model calculation).

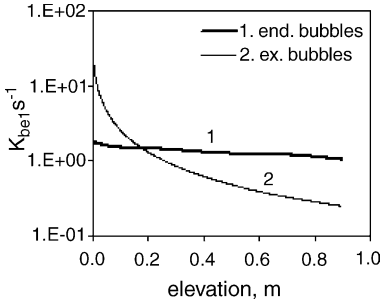


Fig. 6. Coefficient of mass transfer vs. combustor elevation for endogenous and exogenous phases (base case of model calculation).

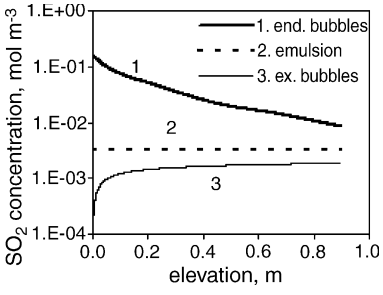


Fig. 7. Concentration of sulfur dioxide in endogenous, exogenous and emulsion phases (base case of model calculation).

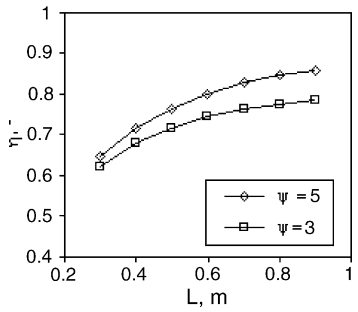


Fig. 8. Desulfurization efficiency vs. bed height for two different Ca/S ratios (model calculations).

steadily decreases by the occurrence of the parallel mechanisms of mass transfer with emulsion and coalescence with fuel lean exogenous bubbles. The exogenous phase is progressively enriched in $SO_2$ as a consequence of the diffusive mass transfer with the emulsion.

Fig. 8 shows the predicted dependence of the desulfurization efficiency on the bed heights. Two data series are reported for different values of the Ca/S ratio (3 and 5). The model correctly predicts the increase of $\eta$ with the bed height, as a consequence of the longer contact time between bubbles and the emulsion. Nevertheless, it is worth noting that increasing $L$ over certain values does not improve considerably the sulfur retention, because the bubbles become too large in size and the mass transfer with the emulsion is depressed.

Fig. 9 shows the dependence of the desulfurization efficiency on Ca/S ratio, for conditions similar to those of the experiments. The model well predicts the increase of $\eta$ with the Ca/S ratio. It also appears that data are approaching an horizontal asymptote for $\Psi > 4$. The comparison with experimental data reported in Fig. 3 is quite satisfactory. In fact, the model predictions are slightly underestimated of about 5% in the range $\Psi = 1$–5. This good figure of the model can be ascribed to the robustness of the adopted assumptions as well as to the accurate evaluation of the parameters for the sulfation kinetics. The neglected contribution to sulfur retention inside the bubbles and in the freeboard region is the major reason of the underestimated model predictions.

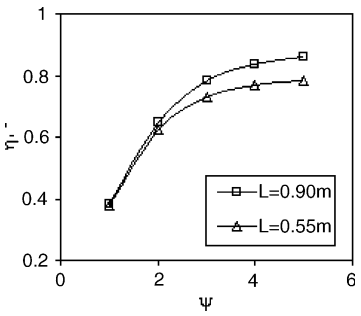


Fig. 9. Desulfurization efficiency vs. Ca/S ratio for different bed heights (model calculations).

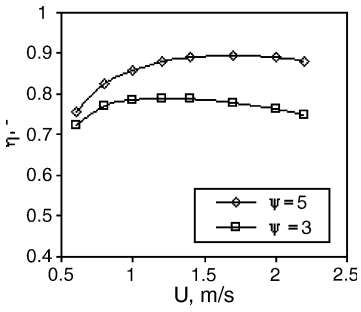


Fig. 10. Desulfurization efficiency vs. fluidization velocity for different Ca/S ratios (model calculations).

Fig. 10 shows the model estimates at different values of the fluidization velocity for two values of the Ca/S ratio (3 and 5). It appears that increasing U leads to a non-monotone change of the desulfurization efficiency that first augments and then decreases. The occurrence of a maximum, the position of which depends on the adopted value of the Ca/S ratio, should be attributed to the combined effect played by the fluidization velocity on the volumetric flow rate of exogenous phase, the size of the exogenous bubbles, and, in turn, the diffusion coefficient between exogenous and emulsion phases. In particular, Eq. (12) gives a non-monotone dependence of the bubble size with $U$, exerting a prominent influence on the model results here presented.

## 6. Conclusions

Combustion and desulfurization tests of a high sulfur liquid fuel (Egyptian mazut) have been performed in a bubbling fluidized bed combustor equipped with a purposely designed fuel injector.

Among operating variables, the focus was on the role played by the bed height, the dispersion flow rate and the Ca/S ratio. The choice of operating variables that minimizes segregation phenomena in the bed is effective to enhance both the combustion efficiency and the sulfur retention. In particular, the rate of dispersion gas used for the fuel injection has a large effect on internal mixing and promotes both fuel conversion and desulfurization.

A predictive mathematical model of FB desulfurization applicable for liquid fuels was purposely developed. The model is based on a novel three phases schematization of the bed. The mechanism of bubble coalescence, the diffusion between bubbles and the emulsion, a global kinetics of sulfatation, a simplified scheme for the fuel conversion in the bed, sorbent attrition and elutriation are considered in this theoretical framework.

The model correctly predicts the trend of the desulfurization efficiency with the explored operating variables (bed height, Ca/S ratio) and slightly underestimates the experimental data. Nevertheless, the model appears to be enough accurate for engineering appliance.

## References


[1] S.C. Saxena, K. Jotshi, Prog. Energy Combust. Sci. 20 (1994) 281–324.
[2] S. Wu, J. Song, K.M. Tuncay, Sellakumar, Proceedings of the 16th International Conference on Fluidized Bed Combustion, Paper FBC01-0185, ASME, Reno Nevada, USA, 2001.
[3] K.K. Pillai, D.E. Elliott, J. Inst. Fuel (1976) 206–210.
[4] V.R. Keler, B.V. Berg, Teploenegetika 10 (1979) 60–62.
[5] Y.P. Enyakin, M.P. Zaitseva, M.N. Maidanic, E.V. Bozhevol'nova, N.S. Maslennekova, A.N. Pozhogina, V.F. Terzieva, Teploenegetika 12 (1980) 33–36.
[6] F. Miccio, M. Miccio, L. Repetto, A. Traniello Gradassi, Proceedings of the 15th International Conference on Fluidized Bed Combustion, ASME, Savannah, USA, 1999, pp. 1354–1376.
[7] D. Barker, B. Beacham, Proceedings of the Inst. of Fuel Inter. Conf., London, UK, 1980, p. I-A3.
[8] B. Beacham, A.R. Marshall, J. Inst. Energy (1979) 59–64.
[9] R. Legros, C.J. Lim, C.M.H. Bretreton, J.R. Grace, Fuel 70 (1991) 1465–1471.
[10] B. North, C. Eleftheriades, A. Engelbrecht, Proceedings of the 15th International Conference on Fluidized Bed Combustion, Paper No. FBC99-0017, ASME, Savannah, USA, 1999.
[11] J. Zhang, D.Y. Lu, E.J. Anthony, Proceedings of the 16th International Conference on Fluidized Bed Combustion, Paper FBC01-0093, ASME, Reno Nevada, USA, 2001.
[12] E.J. Anthony, D.L. Granatstein, Prog. Energy Combust. Sci. 27 (2001) 215–236.
[13] B. Leckner, Prog. Energy Combust. Sci. 24 (1998) 31–61.
[14] M. Fiorentino, A. Marzocchella, P. Salatino, Chem. Eng. Sci. 52 (1997) 1909–1922.
[15] F. Miccio, M. Miccio, G. Olivieri, A. Silvestre, Ind. Eng. Chem. Res. 42 (2003) 3973–3981.
[16] F.M. Okasha, S.H. El-Emam, H.K. Mostafa, Proceedings of the Third Mediterranean Symposium on Combustion, Sharm El-Sheikh, Egypt, 2002, pp. 1087–1098.
[17] D. Kunii, O. Levenspiel, Fluidization Engineering, Butterworths–Heinemann, 1991.
[18] M. Fiorentino, F. Miccio, Combust. Sci. Tech. 159 (2000) 57–86.
[19] P. Cai, M. Schiavetti, G. De Michele, G.C. Grazzini, M. Miccio, Powder Tech. 80 (1994) 99–109.
[20] C.K. Westbrook, F.L. Dryer, Prog. Energy Combust. Sci. 10 (1984) 1–57.
[21] J.S. Dennis, A.N. Hayurst, I.G. Mackley, Proc. Combust. Inst. 19 (1982) 1205–1212.
[22] F. Scala, A. Cammarota, R. Chirone, P. Salatino, AIChE J. 43 (1997) 363–373.